

Transcriptome and Proteome Expressions Involved in Insulin Resistance in Muscle and Activated T-Lymphocytes of Patients with Type 2 Diabetes

Frankie B. Stentz* and Abbas E. Kitabchi

Division of Endocrinology, Diabetes and Metabolism, Department of Medicine, The University of Tennessee Health Science Center, Memphis, TN 38163, USA.

We analyzed the genes expressed (transcriptomes) and the proteins translated (proteomes) in muscle tissues and activated CD4⁺ and CD8⁺ T-lymphocytes (T-cells) of five Type 2 diabetes (T2DM) subjects using Affymetrix microarrays and mass spectrometry, and compared them with matched non-diabetic controls. Gene expressions of insulin receptor (INSR), vitamin D receptor, insulin degrading enzyme, Akt, insulin receptor substrate-1 (IRS-1), IRS-2, glucose transporter 4 (GLUT4), and enzymes of the glycolytic pathway were decreased at least 50% in T2DM than in controls. However, there was greater than two-fold gene upregulation of plasma cell glycoprotein-1, tumor necrosis factor α (TNF α), and gluconeogenic enzymes in T2DM than in controls. The gene silencing for INSR or TNF α resulted in the inhibition or stimulation of GLUT4, respectively. Proteome profiles corresponding to molecular weights of the above translated transcriptomes showed different patterns of changes between T2DM and controls. Meanwhile, changes in transcriptomes and proteomes between muscle and activated T-cells of T2DM were comparable. Activated T-cells, analogous to muscle cells, expressed insulin signaling and glucose metabolism genes and gene products. In conclusion, T-cells and muscle in T2DM exhibited differences in expression of certain genes and gene products relative to non-diabetic controls. These alterations in transcriptomes and proteomes in T2DM may be involved in insulin resistance.

Key words: genomics, proteomics, T-lymphocytes, activation, muscle, Type 2 diabetes

Introduction

T-lymphocytes (T-cells) are unique in that in the native resting state they do not possess insulin receptors (INSRs) and are insulin insensitive; however, within 24 hours after activation with phytohemagglutinin (PHA), T-cells develop receptors for a variety of growth factors such as insulin, insulin-like growth factor 1 (IGF-1), and interleukin-2 (IL-2), which continue to increase in number up to 72 hours (1–5). T-cells also develop certain enzymatic mechanisms for the metabolism of various substrates concomitant with the development of these receptors (4, 5). Our previous studies have demonstrated that insulin binding and responsiveness are reflective of the donor's glycemic status and ambient insulin levels (4, 6, 7), and have shown that the activation of T-cells exhibits

changes in certain transcriptomes and proteomes consistent with metabolic changes noted with their activation (8).

With our studies of *in vivo* activation of T-cells, we noted under hyperglycemic conditions (for example, diabetic ketoacidosis) that there was *in situ* activation with *de novo* emergence of growth factor receptors, such as receptors for insulin, IGF-1, and IL-2 (9). Our *in vitro* studies have demonstrated that the level of activation is glucose concentration and time-dependent (10). This activation is associated with signs of oxidative stress, such as production of reactive oxygen species (ROS), dichlorofluorescein, and lipid peroxidation (as determined by thiobarbituric acid) reactive molecules (11).

In insulin responsive tissues, insulin binds to its receptor and initiates insulin signal transduction pathways. However, cells of patients with Type 2 diabetes

***Corresponding author.**

E-mail: fstentz@utmem.edu

(T2DM) exhibit inhibition of post receptor events and alteration of signal transduction pathways (12–16). Since studies have demonstrated that insulin signal transduction in skeletal muscle, which is an insulin responsive tissue and a major tissue for glucose metabolism, is affected by the level of glucose to which the muscle is exposed (17, 18), we carried out genomic and proteomic analyses on muscle tissues of normal and T2DM subjects. Additionally, since our earlier studies on activated T-cells of normal subjects involving transcriptome and proteome studies appear to be consistent with the changes in muscle tissues (8), we hypothesize that the transcriptomes and proteomes of activated T-cells of T2DM subjects are different from those of normal subjects and are parallel to those of muscle tissues.

Therefore, our aims in this study were: (1) to analyze and compare the genes expressed (transcriptomes) in muscle tissues and activated and non-activated T-cells of normal and T2DM subjects, focusing predominantly on gene alterations in the area of insulin signal transduction and glucose metabolic pathways; and (2) to determine the proteins translated (proteomes) in muscle tissues and activated and non-activated T-cells of normal and T2DM subjects.

Since CD4⁺ and CD8⁺ T-cells exhibit different immunological properties but similar *de novo* emergence of growth factor receptors (5), we studied activated and non-activated CD4⁺ and CD8⁺ T-cells in regard to alteration of gene expression using the Affymetrix human genome microarray chips. We report here significant changes in muscle tissues and activated T-cells of T2DM subjects compared with those of non-diabetic subjects in regard to expression of transcriptomes and proteomes, which may be involved in the insulin resistance of T2DM subjects. To

our knowledge, this is the first report of these phenomena.

Results

Clinical and biochemical data

Table 1 summarizes the clinical and biochemical data on five normal and five diabetic (T2DM) subjects. The diabetic subjects had elevated fasting blood glucose (FBG) and oral glucose tolerance test (OGTT) values indicative of diabetes, as well as an elevated HbA1c percentage. Based on the homeostasis model assessment of insulin resistance (HOMA IR), the normal subjects were not insulin resistant, whereas the diabetic subjects showed marked insulin resistance. It should be noted that these normal male subjects were in good physical condition and good muscle tone, and the body mass index (BMI) is not a good indicator of obesity as also indicated by HOMA IR.

Gene expression

The genes expressed in muscle tissues and activated CD4⁺ and CD8⁺ T-cells in the five newly diagnosed diabetic subjects were compared with those in the five matched (age, gender, ethnicity, and BMI) normal subjects, since neither of the non-activated CD4⁺ or CD8⁺ T-cells showed any growth factor and insulin signaling expression as we have previously reported (8). Figure 1 shows the scatter map of genes increased (red), unchanged (blue), and decreased (green) in activated CD4⁺ T-cells between diabetic and normal subjects. Much more genes were noted to be decreased in expression in diabetic subjects. Similar relationships were also noted in activated CD8⁺ T-

Table 1 Clinical and biochemical characteristics of subjects studied

| Parameter | Normal subjects | Diabetic subjects |
|--|-----------------|-------------------|
| No. of subjects | 5 | 5 |
| Age (year) | 41.2±2.6 | 39.4±2.3 |
| BMI (kg/m ²) | 32.4±2.0 | 34.5±2.4 |
| Temperature (°C) | 37.0±0.08 | 37.0±0.09 |
| HbA1c (%) | 5.2±0.03 | 8.9±0.8 |
| White blood cells (×10 ⁶ /cc) | 5.9±0.6 | 6.3±0.5 |
| FBG (mM) | 5.0±0.2 | 10.5±1.0 |
| Fasting insulin (pM) | 41.4±2.4 | 171.6±14.4 |
| HOMA IR | 1.6±0.2 | 13.4±0.9 |
| Cholesterol level (mg/dL) | 162±14 | 254±33 |
| Triglyceride level (mg/dL) | 126±18 | 223±36 |

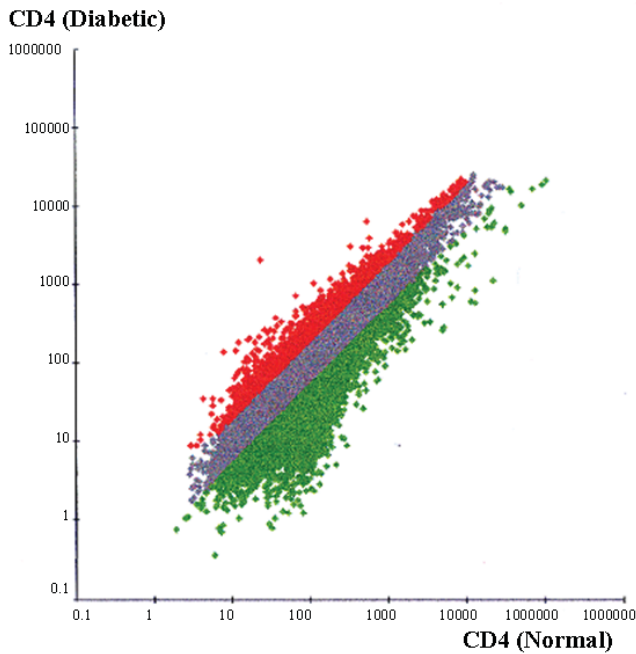


Fig. 1 The scatter map of genes increased (red), unchanged (blue), and decreased (green) in the activated CD4⁺ T-cells of diabetic subjects compared with normal subjects.

cells as well as muscle tissues between diabetic and normal subjects (data not shown). The numerous changes in these cells were grouped into gene ontologies (GOs). Table 2 lists the selected GOs and the number of genes with decreased or increased expression in activated CD4⁺ T-cells of diabetic subjects compared with those of normal subjects. Much more genes were decreased in expression in these GOs of diabetic subjects, especially those for physiological processes, cellular processes, and metabolism.

Figure 2 shows the hierarchical clustering heat map of the genes expressed in activated CD4⁺ T-cells of diabetic subjects in relationship to normal subjects, which are involved in insulin signal transduction (Group 1), inflammation (Group 2), and carbohydrate metabolism (Group 3). Most of the genes involved in these pathways were decreased in diabetic subjects. However, some of the genes were increased in expression in diabetic subjects, including genes of ectonucleotide pyrophosphatase/phosphodiesterase-1 (ENPP-1) or plasma cell glycoprotein-1 (PC-1), Forkhead transcription factor 1 (Foxo1), phosphoenolpyruvate carboxykinase (PEPCK), fructose-1,6-bisphosphatase (FBP), carnitine acyl transferase (CAT), and pyruvate dehydrogenase kinase (isozyme 4) (PDK4). Additionally, inflammatory genes of tumor necrosis factor α (TNF α), TNF α receptor,

Table 2 Gene expression changes grouped by ontologies

| Gene ontology | Decreased in T2DM | Increased in T2DM |
|--------------------------------|-------------------|-------------------|
| Physiological processes | 2,242 | 656 |
| Cellular processes | 1,562 | 368 |
| Development | 556 | 80 |
| Metabolism | 1,419 | 490 |
| Cell growth and/or maintenance | 830 | 262 |
| Response to external stimulus | 401 | 83 |
| Response to stress | 225 | 64 |

and nuclear factor kappa B (NFKB1) were also increased in expression in diabetic subjects, while the T-cell growth factor IL-2, IL-2 receptor (IL-2R), and vitamin D receptor (VDR) were decreased in expression in diabetic subjects.

The differences of the growth factor receptor gene expressions in muscle tissues and activated CD4⁺ and CD8⁺ T-cells were quantitatively compared between normal and diabetic subjects. The directions of changes in gene expression were the same in these patients; they were significantly lower in diabetic subjects than in normal subjects as shown in Figure 3. Table 3 summarizes the fluorescence intensities of the microarray gene chips of some of the genes with changed expression in muscle tissues and activated CD4⁺ and CD8⁺ T-cells of normal and diabetic subjects. Gene expressions of growth factor receptors and enzymes of the glycolytic pathway as well as insulin signal transduction were decreased at least 50% in muscle tissues and activated T-cells of diabetic subjects. In contrast, ENPP-1 (PC-1), associated with diabetes and insulin resistance, was increased to at least two folds in diabetic subjects. PEPCK, involved in the gluconeogenic pathway, was also increased over two folds in diabetic subjects. Significant changes in enzymes involved in signal transduction pathways were noted to be concomitant with the development of insulin insensitivity in these tissues. Table 4 lists the genes and their Unigene IDs that are shown in the hierarchical clustering heat map of Figure 2. The down arrow, up arrow, and horizontal arrow indicate a decrease, increase, or no change, respectively, in the gene expression in diabetic subjects compared with that in normal subjects.

To confirm the gene expression results obtained by the microarrays, quantitative reverse transcription-polymerase chain reaction (RT-PCR) was performed on some of the transcriptomes. Table 5 shows the



Fig. 2 The hierarchical clustering heat map of genes involved in insulin signal transduction (Group 1), inflammation (Group 2), and carbohydrate metabolism (Group 3) in activated CD4⁺ T-cells of diabetic and normal subjects. The green color indicates the genes decreased in expression and the red color indicates the genes increased in expression.

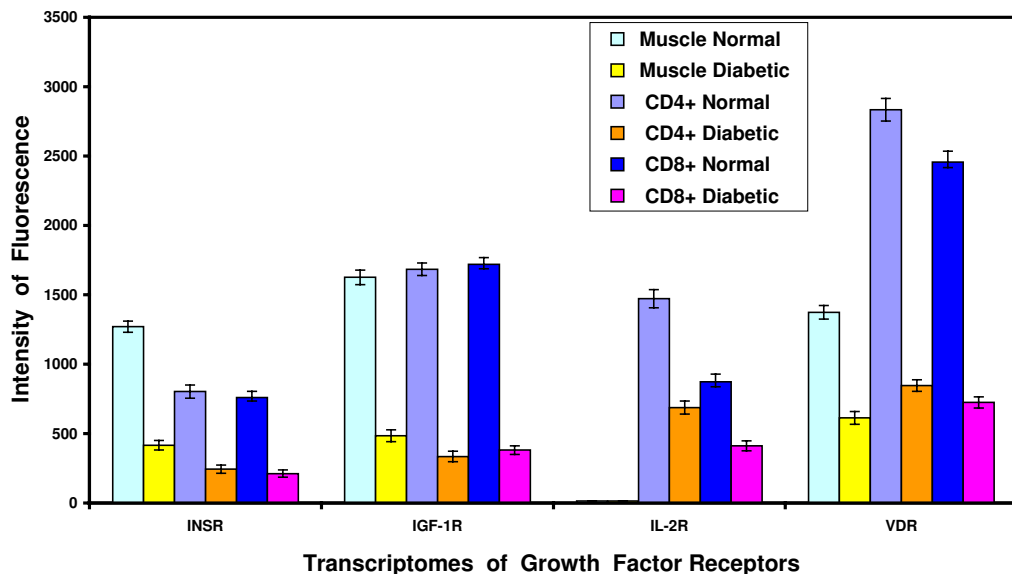


Fig. 3 The growth factor receptor transcriptomes in muscle tissues and activated CD4⁺ and CD8⁺ T-cells of normal and diabetic subjects.

Table 3 Transcriptome levels in muscle tissues and CD4⁺ and CD8⁺ T-cells of normal and diabetic subjects (mean±standard deviation of fluorescence intensities)

| Transcriptome | Muscle | | CD4 ⁺ | | CD8 ⁺ | |
|---------------|----------|-----------|------------------|-----------|------------------|-----------|
| | Normal | Diabetic | Normal | Diabetic | Normal | Diabetic |
| INSR | 1,270±40 | 416±34* | 803±48 | 244±29* | 760±44 | 212±26* |
| IGF-1R | 1,626±52 | 485±43* | 1,684±45 | 335±38* | 1,719±49 | 381±31* |
| IL-2R | 15±1 | 15±1 | 1,472±66 | 687±47* | 873±56 | 412±36* |
| VDR | 1,374±49 | 613±46* | 2,834±51 | 846±42* | 2,457±48 | 724±40* |
| IDE | 1,760±58 | 734±51* | 1,515±44 | 338±39* | 1,382±46 | 296±35* |
| Akt | 1,483±63 | 556±57* | 1,384±76 | 435±48* | 1,270±69 | 389±44* |
| IRS-1 | 1,940±65 | 810±55* | 1,474±63 | 578±52* | 1,328±67 | 631±56* |
| IRS-2 | 1,237±60 | 621±52* | 1,314±68 | 652±58* | 1,194±65 | 588±47* |
| HK | 2,786±94 | 1,191±67* | 2,254±91 | 964±67* | 2,382±86 | 1,012±64* |
| PFK | 3,634±71 | 872±58* | 3,286±81 | 647±72* | 2,974±74 | 583±58* |
| PDH | 1,543±61 | 719±63* | 1,062±76 | 453±49* | 893±73 | 415±44* |
| ENPP-1 | 818±46 | 1,760±59* | 764±51 | 1,657±60* | 703±53 | 1,564±59* |
| GLUT4 | 1,286±67 | 591±52* | 615±58 | 273±36* | 562±57 | 241±34* |
| GAPD | 2,858±84 | 1,406±79* | 2,285±93 | 1,037±64* | 1,974±90 | 964±61* |
| CALM | 2,012±54 | 804±46* | 1,647±44 | 715±47* | 1,792±61 | 689±53* |
| PEPCK | 685±42 | 2,033±57* | 591±39 | 1,872±52* | 495±38 | 1,708±59* |

*Significant difference ($p < 0.05$) between normal and diabetic subjects. HK, hexokinase; PFK, phosphofructokinase; PDH, pyruvate dehydrogenase; GAPD, glyceraldehyde-3-phosphate dehydrogenase; CALM, calmodulin.

Table 4 Identification of genes expressed in activated CD4⁺ T-cells of diabetic subjects

| Gene ID | Identification | Expression |
|-----------|--|------------|
| Hs.465744 | Insulin receptor (INSR) | ↓ |
| Hs.500546 | Insulin degrading enzyme (IDE) | ↓ |
| Hs.487062 | Insulin-like growth factor-2 receptor (IGF-2R) | ↓ |
| Hs.20573 | Insulin-like growth factor-1 receptor (IGF-1R) | ↓ |
| Hs.471508 | Insulin receptor substrate-1 (IRS-1) | ↓ |
| Hs.442344 | Insulin receptor substrate-2 (IRS-2) | ↓ |
| Hs.525622 | Akt/Protein kinase B (PKB) | ↓ |
| Hs.15744 | SH2-B homolog | ↓ |
| Hs.464971 | Phosphoinositide-3-kinase (PI3K) | ↓ |
| Hs.104123 | Phosphoribosyl pyrophosphate synthetase 3 | ↓ |
| Hs.123253 | SHC SH2 domain binding protein 1 | ↓ |
| Hs.531704 | Protein kinase C | ↓ |
| Hs.282410 | Calmodulin | ↓ |
| Hs.513661 | Mitogen act protein II | ↓ |
| Hs.203420 | Tyrosine kinase I | ↓ |
| Hs.408312 | Tumor protein p53 | ↓ |
| Hs.159161 | Rho GDP dissociation inhibitor (GDI) | ↓ |
| Hs.505469 | Rac (GTPase activating protein) | ↓ |
| Hs.518355 | G-elongation factor (mito 1) | ↓ |
| Hs.369779 | Sirtuin1 (SIRT1) | ↓ |
| Hs.397729 | HMGCoA synthase (HMGCS1) | ↔ |
| Hs.103854 | Dock protein 1 (downstream of tyrosine kinase 1) | ↓ |
| Hs.431850 | MAP kinase (ERK) | ↓ |
| Hs.463642 | Ribosomal protein kinase S6 | ↓ |

Table 4 *Continued*

| Gene ID | Identification | Expression |
|-----------|--|------------|
| Hs.431498 | Foxo1 | ↑ |
| Hs.458285 | SH3 domain (GRB3-like 2) | ↓ |
| Hs.487897 | Phosphodiesterase (PDE1C) | ↓ |
| Hs.524461 | SP1 | ↓ |
| Hs.162646 | Peroxisome proliferative activated receptor γ | ↓ |
| Hs.527295 | ENPP-1 | ↑ |
| Hs.413513 | Inhibitor kinase (I kappa B) | ↓ |
| Hs.89679 | Interleukin-2 (IL-2) | ↓ |
| Hs.231367 | IL-2 receptor (IL-2R) | ↓ |
| Hs.401745 | TNF α receptor 2 | ↑ |
| Hs.478275 | TNF α | ↑ |
| Hs.524368 | Vitamin D receptor (VDR) | ↓ |
| Hs.431926 | Nuclear factor kappa B (NFkB1) | ↑ |
| Hs.466471 | Glucose phosphate isomerase | ↓ |
| Hs.479728 | Glyceraldehyde-3-phosphate dehydrogenase (GAPD) | ↓ |
| Hs.444422 | Pyruvate dehydrogenase kinase (isoenzyme 4) (PDK4) | ↑ |
| Hs.513490 | Aldolase A | ↓ |
| Hs.75160 | Phosphofructokinase (PFK) | ↓ |
| Hs.464071 | Phosphogluconate dehydrogenase | ↓ |
| Hs.171499 | Diacylglycerol kinase | ↓ |
| Hs.131255 | Ubiquinol-Cyto C reductase binding protein (UQCRB) | ↓ |
| Hs.61255 | Fructose-1,6-biphosphatase 2 (FBP) | ↑ |
| Hs.2795 | Lactate dehydrogenase A | ↓ |
| Hs.148266 | Glycerol-3-phosphate dehydrogenase 2 (mito) | ↓ |
| Hs.546323 | Succinate-CoA ligase (ADP forming B sub) | ↓ |
| Hs.12068 | Carnitine acyl transferase (CAT) | ↑ |
| Hs.199776 | Potassium inwardly rectifying channel, subfam 3-6 | ↔ |
| Hs.430606 | Citrate synthase | ↓ |
| Hs.530274 | Aldolase B, fructose-biphosphate | ↓ |
| Hs.517145 | Enolase 1 | ↓ |
| Hs.413238 | Phosphoglycerate mutase 1 | ↓ |
| Hs.154654 | Cytochrome p450 family subunit B | ↓ |
| Hs.83765 | Dihydrofolate reductase | ↓ |
| Hs.406266 | Hexokinase-2 (HK) | ↓ |
| Hs.567249 | Soluble carrier family 2 (fac glu trans) mem 4 (GLUT4) | ↓ |
| Hs.1872 | Phosphoenolpyruvate carboxykinase (PEPCK) | ↑ |
| Hs.358935 | Soluble carrier family 5 (Na/glu cotrans) mem 10 | ↓ |
| Hs.524219 | Triosphosphate isomerase | ↔ |
| Hs.130036 | Protein phosphatase 1 | ↓ |
| Hs.198281 | Pyruvate kinase, cGMP dependent, type 1 | ↓ |
| Hs.151176 | AcetylCoA carboxylase | ↓ |
| Hs.530331 | Pyruvate dehydrogenase (PDH) | ↓ |

gene expression comparison results of 23 genes selected from the list of genes in Table 4. The mRNA levels of normal subjects were compared with those of diabetic subjects for the respective tissues using the factor $\Delta\Delta C_{t_{test\ gene}}$. The larger the $\Delta\Delta C_{t_{test\ gene}}$,

the less the amount of mRNA in diabetic subject cells than in normal subject cells. The negative values indicate increased expression of mRNA in diabetic subjects than in normal subjects, which confirms the increased expression of these genes (FBP, PEPCK,

Table 5 Changes in gene expression determined by quantitative RT-PCR

| Gene expression | $\Delta\Delta\text{Ct}$ | | |
|--|-------------------------|------------------|------------------|
| | Muscle | CD4 ⁺ | CD8 ⁺ |
| GAPD | 1.8 | 1.6 | 1.5 |
| PFK | 2.6 | 2.3 | 2.3 |
| FBP | -1.9 | -1.8 | -1.8 |
| HK | 1.9 | 1.7 | 1.6 |
| GLUT4 | 1.5 | 1.5 | 1.5 |
| PEPCK | -2.5 | -2.2 | -2.2 |
| Soluble carrier family 5 (Na/glu cotrans) mem 10 | 0.7 | 0.6 | 0.6 |
| PDH | 1.6 | 1.5 | 1.4 |
| CAT | -1.2 | -1.1 | -1.1 |
| INSR | 1.8 | 1.9 | 1.9 |
| IDE | 2.2 | 1.7 | 1.6 |
| IGF-1 | 1.9 | 2.3 | 2.2 |
| IRS-1 | 1.6 | 1.7 | 1.6 |
| Akt | 1.7 | 1.9 | 1.8 |
| Calmodulin | 1.6 | 1.5 | 1.5 |
| PDK4 | -1.3 | -1.2 | -1.2 |
| Foxo1 | -1.4 | -1.3 | -1.1 |
| PDE1C | 1.6 | 1.5 | 1.5 |
| SP1 | 1.4 | 1.3 | 1.3 |
| ENPP-1 | -1.5 | -1.4 | -1.4 |
| IL-2R | 0 | 1.6 | 1.6 |
| NFKB1 | -1.4 | -1.5 | -1.6 |
| VDR | 1.7 | 2.3 | 2.1 |
| 18S rRNA | - | - | - |

CAT, PDK4, Foxo1, ENPP-1, and NFKB1) observed with the Affymetrix microarrays in diabetic subjects.

Figure 4 shows the percent relative gene expression determined when RNA interference (RNAi) was used for gene knockout to study the effect of mRNA expression levels. The CD4⁺ T-cells of normal subjects were transfected with Silencer siRNAs before activation of the cells, and the mRNA knockout levels were measured. Using 1 nM and 10 nM concentrations of INSR siRNAs resulted in a decrease and almost total knockout of the mRNA levels for INSR and glucose transporter 4 (GLUT4), respectively. Using 1 nM and 10 nM concentrations of TNF α siRNAs resulted in a decrease and almost total knockout of the mRNA levels for TNF α , respectively, but an increase in the mRNA levels for GLUT4 (data not shown). 18S rRNA was used to normalize from sample to sample.

Proteomics analysis

To further evaluate the nature of the proteomic changes, total cellular proteins from muscle tissues

and activated and non-activated CD4⁺ and CD8⁺ T-cells of normal and diabetic subjects were analyzed using two-dimensional polyacrylamide gel electrophoresis (2D-PAGE) and mass spectrometry (MS). Figure 5 (A and B) shows the 2D gel profiles of activated CD4⁺ T-cells of diabetic and normal subjects, respectively, with pI ranging from 3 to 10 for the first dimension. This demonstrates the numerous changes in proteins between diabetic and normal CD4⁺ T-cells. Numerous differences between diabetic and normal CD8⁺ T-cells and muscle tissues were also observed (data not shown).

Because of the large number of differences in protein spots on the 2D gels and the large number of samples to be analyzed in this study, the muscle tissues and activated CD4⁺ and CD8⁺ T-cells of diabetic and normal subjects were analyzed on a Beckman Coulter ProteomeLab PF 2D Protein Fractional System (Figure 5C). The protein peaks were compared between diabetic and normal subjects (Figure 5D). The collected protein peaks were then subjected to further analysis by matrix-assisted laser desorption/ionization

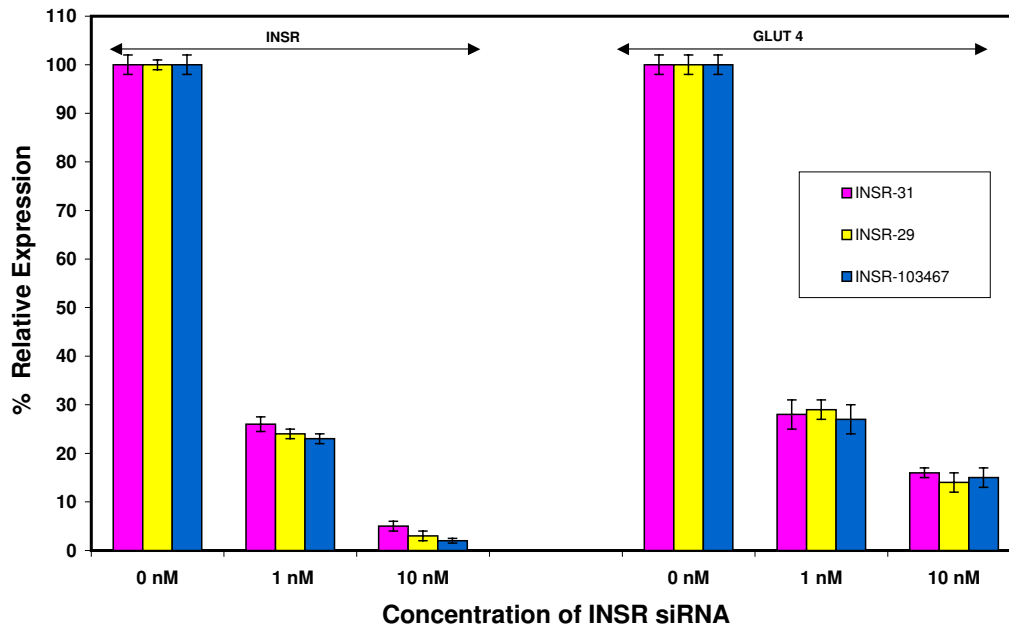


Fig. 4 The effect of gene silencing of mRNAs for INSR and GLUT4 using siRNAs for INSR.

time-of-flight (MALDI-TOF) MS.

Figure 6 (A and B) shows the mass spectrometric profiles in the m/z range of 100–30,000 and 30,000–150,000, respectively, using the gold metal microarrays on a CIPHERGEN PBSII surface-enhanced laser desorption/ionization time-of-flight (SELDI-TOF) mass spectrometer with CIPHERGEN ProteinChip 3.1 and Biomarker Wizard software. As can be seen from the figure, there are numerous differences in protein patterns of activated T-cells between normal and diabetic subjects. These differences appear to correlate with the numerous differences observed in the transcriptomes of activated and non-activated T-cells between normal and diabetic subjects as well as in the proteins observed with 2D-PAGE. It is proposed that some of these proteins may serve as biomarkers in T2DM during their cell activation. Table 6 shows some of these possible biomarkers for the activation of CD4⁺ T-cells and muscle tissues for T2DM in the m/z range of 500–150,000, which were determined from the MS peak map data analysis of the triplicate samples of normal and diabetic subjects. Proteins with these m/z values were determined to be either unique or were increased or decreased significantly in concentration in activated CD4⁺ T-cells or muscle tissues of diabetic subjects compared with those of normal subjects. For example, the peak intensity of the m/z value of 119,700 was decreased in CD4⁺ T-cells and muscle tissues of diabetic subjects. This m/z value may correspond to the insulin degrading enzyme (IDE) since its transcriptome was deter-

mined to be decreased in expression in diabetic subjects. On the other hand, the peak intensity of the m/z value of 110,000 was increased in diabetic subjects; the m/z values of 15,642, 16,721, and 17,356 were present in diabetic subjects but not in normal subjects; and the peak intensity of the m/z value of 21,148 was decreased in diabetic subjects. Additionally, the peak intensity of the m/z value of 27,714 was decreased in CD4⁺ T-cells of diabetic subjects, and the peak intensity of the m/z value of 27,741 was also decreased in muscle tissues of diabetic subjects. Further mass spectrometric studies need to be done to identify these proteins.

Relationship of transcriptomes in cellular function

Forty-four genes that were altered in expression between normal and diabetic subjects were analyzed by Ingenuity software using GOs and KEGG (Kyoto Encyclopedia of Genes and Genomes) pathways. Table 7 shows the biological profiling of these 44 genes (bold), which are clustered into 3 groups with integration of their functional pathways, together with other genes (non-bold) that are also involved in these pathways. In Group I, 17 of these genes (bold), such as INSR and insulin receptor substrate-1 (IRS-1), are linked with other genes (non-bold) with the main function of carbohydrate metabolism and cell signaling. In Group II, another 13 genes that were altered in expression

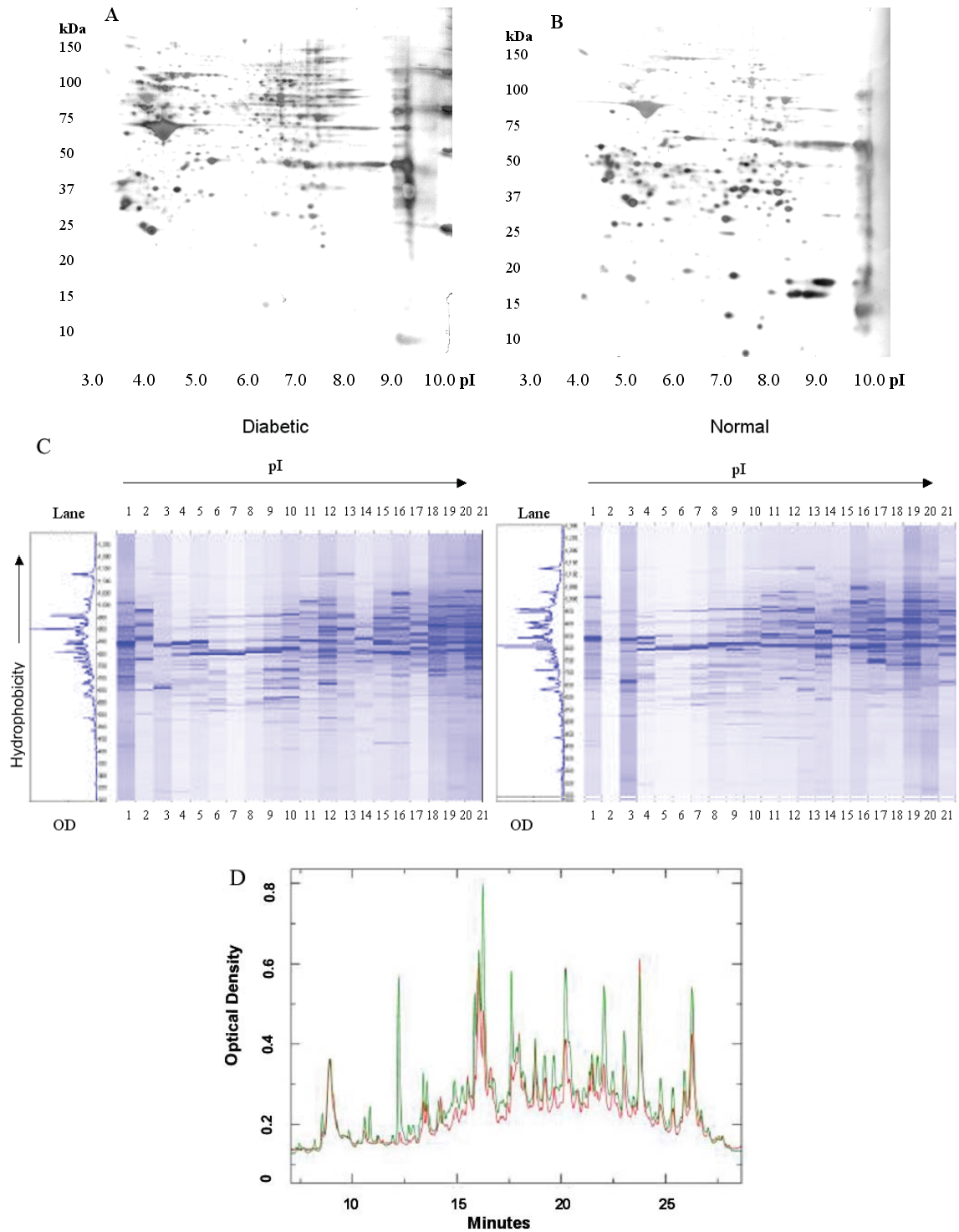


Fig. 5 A and B. The 2D gel profiles of activated CD4⁺ T-cells of diabetic and normal subjects, respectively, with pI ranging from 3 to 10 for the first dimension. C. Analysis of the above activated CD4⁺ T-cells of diabetic and normal subjects using the Beckman Coulter ProteomeLab PF 2D Protein Fractional System by isoelectric focusing and reverse phase separation of proteins. D. The protein peaks were compared between diabetic (red) and normal (green) subjects.

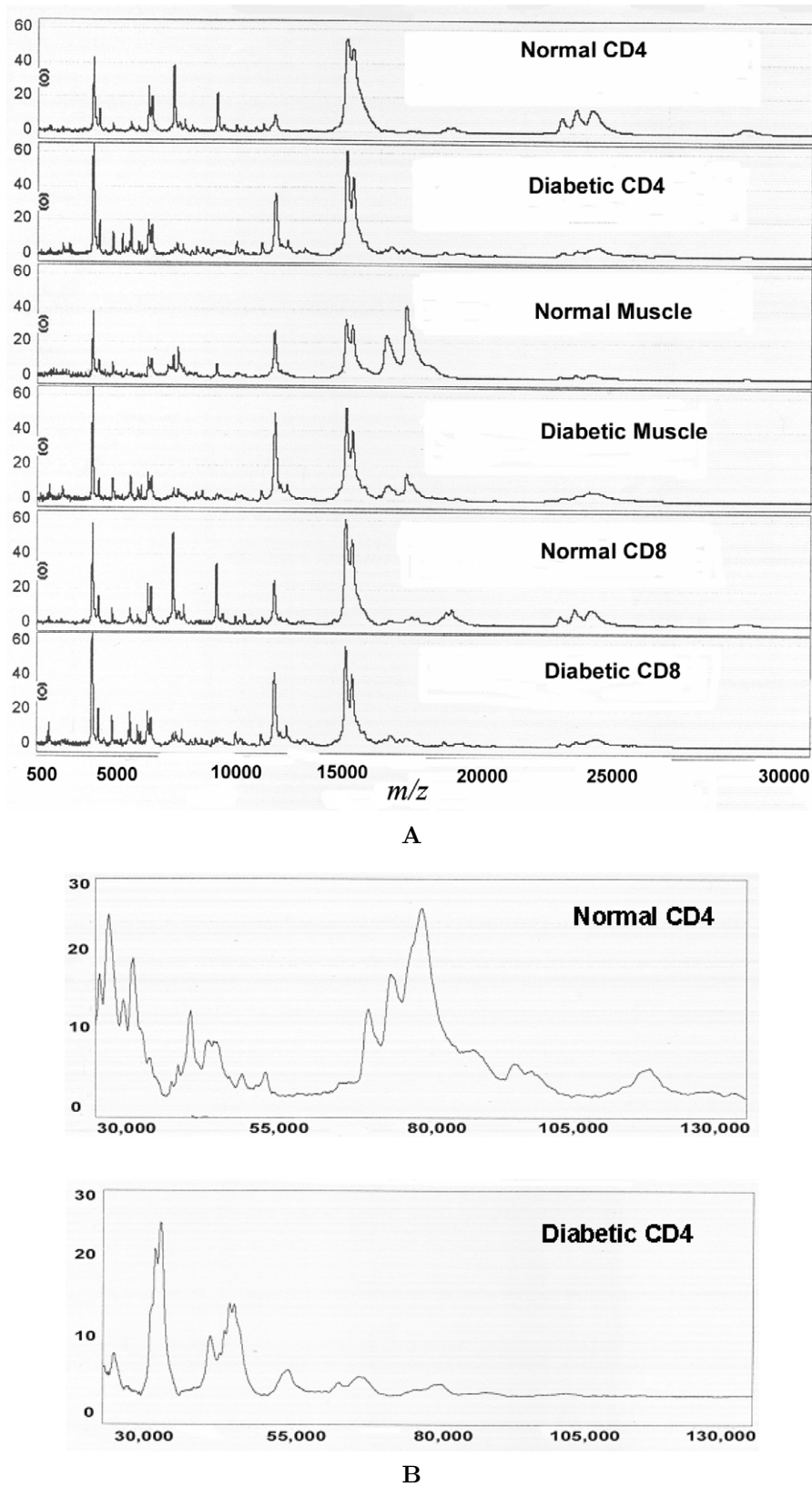


Fig. 6 A. SELDI-TOF MS profiles of muscle tissues and CD4⁺ and CD8⁺ T-cells of normal and diabetic subjects in the m/z range of 100–30,000. **B.** SELDI-TOF MS profiles of CD4⁺ T-cells of normal and diabetic subjects in the m/z range of 30,000–150,000.

Table 6 Potential biomarkers for diabetes in CD4⁺ T-cells and muscle tissues

| Normal | | Diabetic | |
|---------------------------------|-----------------------|---------------------------------|-----------------------|
| CD4 ⁺ (<i>m/z</i>) | Muscle (<i>m/z</i>) | CD4 ⁺ (<i>m/z</i>) | Muscle (<i>m/z</i>) |
| 3,459 | 3,366 | – | 3,366 |
| 3,903 | 3,903 | 3,433 | – |
| 4,154 | 3,481 | 4,154 | 3,481 |
| 5,979 | 3,881 | 5,979 | 3,881 |
| 6,650 | 6,654 | 6,650 | 6,654 |
| 7,760 | 7,771 | 7,760 | – |
| 8,769 | 8,786 | 8,760 | 8,786 |
| 9,276 | 9,295 | 9,276 | – |
| 10,617 | – | 10,617 | – |
| 10,846 | 10,845 | – | 10,845 |
| 11,714 | 11,732 | 11,714 | – |
| 13,210 | – | 13,210 | – |
| – | – | 15,642 | 15,642 |
| – | – | 16,721 | 16,721 |
| – | – | 17,356 | 17,356 |
| 21,148 | 21,148 | 21,148 | 21,148 |
| 22,356 | 22,356 | 23,467 | 23,467 |
| 27,714 | 27,741 | 27,714 | 27,741 |
| 110,000 | 110,000 | 110,000 | 110,000 |
| 119,700 | 119,700 | 119,700 | 119,700 |

Table 7 Ingenuity biological profiling of genes altered in expression in diabetic subjects

| Genes | Focus genes | Top functions |
|---|-------------|--|
| INSR, IRS1, IRS2, IRS4, PEPCK, IL2, GAPD, PDK1, PDK2, PFK, IL2RB, IGF1R, ENPP1, Foxo1, GLUT4, JAK1, VDR, AHSG, ATP2A3, CAV3, CD276, CX3CR1, FER (tyrosine kinase), IFNG, IL2RA, MICA, NCR1, NISCH, PAEP, PDCD1, PD-CDILG2, PDE4B, PHIP, SLC2A4, TXX, VTCN1 | 17 | Carbohydrate metabolism, molecular transport, small molecule biochemistry, cell signaling |
| AKT3, CALM2, G6PD, HK3, IPF1, LDHA, LDHB, PDE1C, PDHB, PDHE, PDK4, PIP5K3, FBP, CART, CNN2, CTNNB1, Cyp2d10, DLAT, DLD, GNPAT, GPAM, INS1, KCNJ1, LEP, LTC45, MAFA, MF12, OAT, PDE3B, PDHA1, PDHA2, PL53, PRKAA1, TAXIBP3, TGFB1 | 13 | Carbohydrate metabolism, small molecule biochemistry, lipid metabolism |
| CALM1, H6PD, HK1, HK2, IDE, INSIG1, CAT, LDHC, PDE1A, PDE1C, PKM2, SP1, TNFα, TNFR, AEBP1, CCRN4L, CD18, CD1C, CLA, CTLA2A, EPHB4, GPAM, HGF, HRSP12, ICOSLG, IFI203, IFIT3, IL4, KITLG, LTC45, MAT2A, MTPN, NFIX, RNF128, SLC29A1 | 14 | Hepatic system, cardiovascular system development and function, cell-to-cell signaling and interaction |

are grouped and linked with genes involved in carbohydrate and lipid metabolism. The other 14 genes are linked in the third group with genes involved in the hepatic and cardiovascular systems and cell-to-cell

signaling. Figure 7 shows the merging of these pathways to integrate the interaction of different pathways of the three groups of these genes and their relationship with other genes that are also involved in these

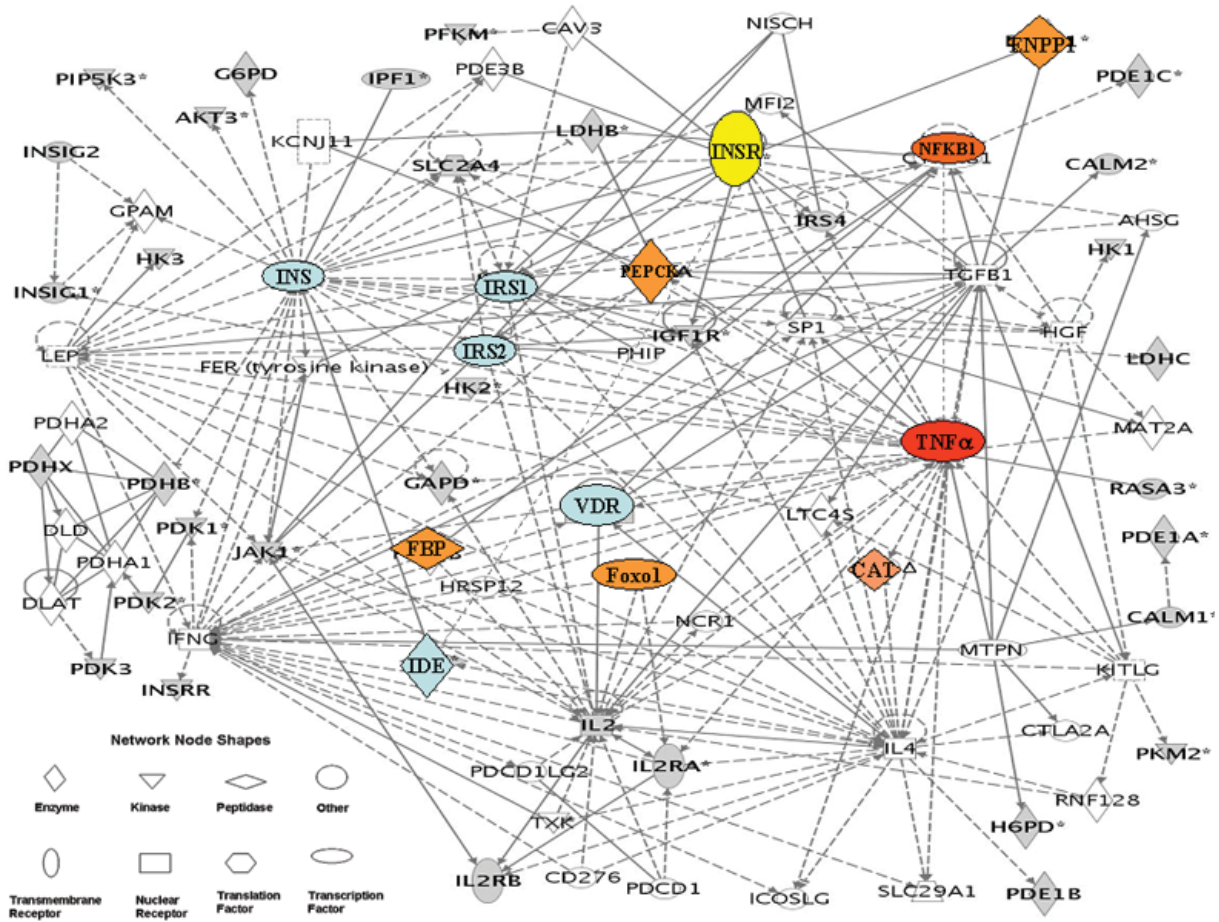


Fig. 7 The merged pathway interactions using Ingenuity software of some of the genes found to be altered between normal and diabetic subjects and the interactions of other genes involved with these pathways.

pathways. This demonstrates the relationship between certain enzymes of intracellular pathways that are affected in T-cells and muscle tissues, and shows the complexity of the relationship between the genes expressed and their far reaching effect on other parts of the system. It also indicates that the alteration in expression of these genes in diabetic subjects can lead to the alteration of numerous pathways and physiological processes involved in T2DM.

Discussion

Our results indicate the expansive effect of elevated glucose in the disease state of T2DM on gene expression with the main focus on carbohydrate metabolism and insulin signaling along with the relationship with inflammation. Based on many studies, the insulin binding to its receptor in insulin-sensitive tissues results in activation of multiple IRSs and numerous enzymes involved in insulin signal transduction (12–15,

19–25). Using the human genome microarrays, we have demonstrated the relationship of numerous genes that were increased or decreased in T2DM.

In this study, the transcriptome for INSR was decreased in diabetic subjects compared with that of normal subjects, so were the transcriptomes for IRS-1 and IRS-2 (Figure 2). Although our 2D-PAGE, PF 2D, and MS analyses for the translation of the proteome were inconclusive, the SELDI-TOF MS profile (Figure 6) showed peaks in the range of the molecular weights (MWs) of IRS-1 (131,591 Da) and IRS-2 (137,334 Da). We have previously shown that the activation of T-cells with high glucose or saturated fatty (palmitic) acids activates the *de novo* expression of INSR on the cell surface of T-cells (4, 9, 11, 26) and increases IRS-1 and IRS-2 (5, 11, 26). However, these expressions were decreased in diabetic subjects (9). Such a decrease of IRS-1 and IRS-2 in diabetic subjects would impair insulin signaling, glucose transport and metabolism, lipid metabolism, and protein synthesis.

IDE has been shown to be an important enzyme involved in insulin sensitivity (27–31). Our results demonstrated that the IDE transcriptome in muscle tissues and activated CD4⁺ and CD8⁺ T-cells was decreased in expression in diabetic subjects. Mass spectrometric characterization of proteins on the SELDI-TOF MS data indicated a protein (proteins) with an m/z value of 119,700, which is approximate to the MW of IDE. The peak intensity was decreased in diabetic subjects, which correlates with our earlier findings (27).

Central within the insulin signaling cascades are many protein kinases. One of these activated protein kinases is Akt (also known as protein kinase B). Activated Akt has many targets, including glucose transport pathways, potassium transport pathways, and protein metabolism. Another major protein kinase is p38 MAPK. The targets of p38 MAPK are less well-established, but are thought to also include glucose transport pathways, potassium transport pathways, and protein metabolism. Although both human and animal studies indicate that the Akt and p38 MAPK pathways are affected in T2DM, the specific role that hyperglycemia has on signal transduction by these pathways is not known (18, 32, 33). Our results presented here corroborate these findings by demonstrating particular differences in gene expression between diabetic and non-diabetic subjects in insulin signal transduction genes, such as Akt3 and IRS-1, as well as in the emergence of growth factor receptors (INSR, IGF-1R, and IL-2R). Additionally, the differences in the MW range of Akt3 (54,032 Da) in the SELDI-TOF MS profile were observed. These findings in CD4⁺ or CD8⁺ T-cells are parallel to those in muscle tissues with respect to many of the transcriptomes and proteomes, indicating that these tissues behave similarly in normal or diabetic subjects and could be used interchangeably for T2DM studies since T-cells are more readily accessible than muscle tissues.

This study further extends the findings in muscle tissues of diabetic and normal subjects by comparing microarray data of genomic and proteomic expression in both T-cells and muscle tissues. Activated CD4⁺ and CD8⁺ T-cells, analogous to muscle cells, express insulin signaling and glucose metabolism genes and gene products. Muscle tissues and activated T-cells of diabetic subjects exhibit less than half of the expression of genes and gene products in numerous pathways compared with those of normal subjects. One of our interesting findings is that the gene expression of ENPP-1, a membrane protein that has been shown

to be increased in diabetes and insulin resistance by Maddux and Goldfine (34), was increased in T-cells and muscle tissues of diabetic subjects to be at least two folds of that in normal subjects. Extending these genomic studies to the proteome level with MS analysis revealed a protein of 110,000 m/z , which was increased in diabetic subjects within the MW range of the ENPP-1 protein. Therefore, we propose that some transcriptome and proteome changes may be involved in the insulin resistance of diabetic subjects relative to normal subjects.

The hierarchical clustering heat map classifies some of the genes altered in expression between normal and diabetic subjects into insulin signal transduction, carbohydrate metabolism, and inflammation. The inflammatory genes of TNF α , TNF α receptor, and NF κ B1 were increased in expression in diabetic subjects, supporting the concept that inflammation is linked to insulin resistance. Although TNF α was much more expressed in T-cells than in muscle tissues, it showed a similar relationship of increase in both T-cells and muscle tissues in diabetic subjects. SELDI-TOF MS showed differences in peaks in the MW range of TNF α and TNF α receptor (17,270 Da and 35,478 Da), respectively, with increase in diabetic subjects. These levels correlate with the previous studies that have shown increased blood levels of TNF α in diabetic subjects (10, 35) and other studies with diabetic animals (36).

The T-cell growth factor IL-2 and IL-2R were decreased in expression in T-cells of diabetic subjects, whereas neither was present in muscle tissues of normal or diabetic subjects. SELDI-TOF MS showed differences in peaks in the MW range of IL-2 and IL-2R (17,628 Da and 30,819 Da), respectively, with decreased peak heights in T-cells of diabetic subjects while none was observed in muscle tissues, as we have reported in our flow cytometry and tissue immunohistochemistry studies (5, 8, 11).

Our results showed that the VDR gene expression was decreased in diabetic subjects. SELDI-TOF MS showed differences in peak heights in the MW range of VDR (48,289 Da) between diabetic and normal subjects. VDR has been shown to be an important anti-inflammatory agent (37, 38), therefore, it may have important implications in the increased infections in diabetic subjects.

The diabetic state is associated with increased gluconeogenesis. Our results showed that two of the rate-limiting enzymes of gluconeogenesis, FBP and PEPCK, as well as the ketogenic enzyme and CAT,

were increased in expression in T-cells and muscle tissues of diabetic subjects. SELDI-TOF MS showed differences in peak heights in the MW range of FBP, PEPCK, and CAT (37,188 Da, 69,195 Da, and 70,926 Da), respectively. The increase of these enzymes would result in an increase of blood glucose and ketone levels in diabetic subjects. The gene expression of the transcription factor Foxo1, which is involved in carbohydrate metabolism, was also increased in T-cells and muscle tissues of diabetic subjects. SELDI-TOF MS showed differences in peak heights in the MW range of Foxo1 (69,662 Da). These findings corroborate the findings of increased Foxo1 in diabetes by Nakae *et al* (39).

These transcriptome and proteome expression results seem to corroborate a number of the proteomic results that have been observed by immunoassay, flow cytometry, and immuno blotting in our previous studies. However, due to the fact that SELDI-TOF MS does not specifically identify a protein but only make a comparison of the MS profile over the m/z range, further 2D separation electrophoresis and MALDI-TOF MS studies are needed for identification of each protein.

For the 23 picked transcriptomes that were found to be altered between normal and diabetic subjects, quantitative RT-PCR confirmed the directional changes of these transcriptomes observed from microarray data, suggesting that microarray data are reliable to express the relationship of gene expression between normal and diabetic subjects.

The microarray data showed decreased expression of INSR and GLUT4 and increased expression of TNF α in diabetic subjects. When gene silencing was used to study the effect of the silencing of INSR on the glucose transport by determining the expression of GLUT4, we found that decreasing the expression of INSR also resulted in a decrease in the GLUT4 expression. However, decreasing the expression of TNF α by gene silencing resulted in an increase in the GLUT4 expression. Thus, this demonstrates the effect of INSR and TNF α on regulating glucose transport and metabolism, as well as the effect of the expression of one gene on the expression of another as shown in Figure 7. When these transcriptomes along with other transcriptomes (Table 7) were analyzed by Ingenuity software, they were shown to be also involved in the hepatic and cardiovascular systems as well as carbohydrate and cell signaling systems. When the genes of these functions were merged (Figure 7), the intricate relationship can be seen be-

tween a gene expression and how it could affect other genes involved in these functions.

It has been shown that activated T-cells along with activated human aortic endothelial cells (HAECs) play a pivotal role in the development of atherogenic plaques (40, 41). We have recently shown that glucose or palmitic acids can activate both HAECs and T-cells with production of ROS, lipid peroxidation, and generation of proinflammatory cytokines and insulin signal transduction intermediates (11, 26, 42). The elevated glucose and palmitic acids as occurred in T2DM on T-cell activation play an important role in the atherogenic plaque formation; therefore, inhibition of the activation through part of the signal transduction mechanism could prevent the T-cell activation and plaque formation.

Our present study used PHA to activate T-cells and study the patterns of genomic and proteomic expressions, and we assume that similar patterns would be observed when these cells are activated with glucose or palmitic acids, as would be encountered in *in vivo* conditions. However, we cannot state with certainty the exact pattern of changes in genomic and proteomic expressions under such *in vivo* conditions, but such studies are needed for verification of the changes between diabetic and non-diabetic subjects. Additionally, our studies were performed on diabetic and non-diabetic African American subjects. Since there are significant phenotypic differences between African American and Caucasian subjects, these studies need to be further verified on Caucasian subjects.

Conclusion

We conclude that there are significant differences in genomic and proteomic patterns of activated T-cells between diabetic and non-diabetic subjects, and these findings parallel our *in situ* findings in muscle tissues of diabetic and non-diabetic subjects. Further studies should be conducted using T-cells, which are more readily available than muscle. Besides, T-cells are important in that they are intricately involved in the immune system and inflammation, and also play a pivotal role in plaque formation and cardiovascular disease, which is a major complication of T2DM (40). Although the diabetic subjects in this study were newly diagnosed and has not yet developed currently observable complication of diabetes such as retinopathy, nephropathy, and neuropathy, the alterations in the transcriptome and proteome expressions

in CD4⁺ and CD8⁺ T-cells and muscle tissues of diabetic subjects compared with those in normal subjects demonstrate that tissue changes were already occurring. These and additional studies could help delineate biomarkers to identify subjects who may have T2DM and lead to the development of therapeutic interventions targeting such affected genes and preventing complications due to diabetes.

Materials and Methods

Subject selection

Five male subjects with newly diagnosed T2DM and five non-diabetic controls were selected for the study, who were matched for BMI (28–40), age (30–56), and ethnicity (African American). They had no history of systemic or metabolic diseases and were on no medications. The diabetic subjects had normal chemistry profiles except high glucoses and were free of microangiopathy, and had no history of macrovascular diseases or other complications associated with T2DM. These subjects were enrolled into the study after signing the consent form approved by the University of Tennessee Health Science Center institutional review board. Assessment of glycemic control was done by a 2-hour OGTT of 75 g dextrose ingestion after 3 days of high carbohydrate diet according to the American Diabetes Association (ADA) criteria (43). All subjects had normal complete blood count (normal range of white blood cells) with no indication of infection or inflammation.

Sample collection and laboratory processing

Blood samples (70 mL) of the studied subjects were obtained in EDTA from an antecubital vein after an overnight fast. The plasma was used for hormone and metabolite measurements. The buffy coat was used for isolation of the peripheral blood leukocytes (PBLs). Muscle biopsies were obtained from the vastus lateralis muscle (thigh muscle). Following local anesthesia (mepivacaine chloride 5 mg/mL), a 5-mm incision in the skin and muscle fascia allowed for 100–200 mg muscle biopsy to be obtained with a Weil-Blakesley conchotome. Each biopsy was immediately placed in 1 mL of TRIZOL reagent (Invitrogen, Carlsbad, USA) and was homogenized (8).

Isolation of CD4⁺ and CD8⁺ T-cells

PBLs were isolated by centrifugation of 70 mL of whole blood at 500×g for 10 min. The upper layer of plasma was removed. The buffy coat was then removed, diluted to 30 mL with phosphate buffered saline (PBS; 0.1% human serum albumin, pH 7.4), layered over Ficoll-Hypaque, and centrifuged. The band of PBLs was then washed with PBS. The CD4⁺ and CD8⁺ T-cells were isolated from the PBLs by negative selection using the CD4 and CD8 lymphocyte negative isolation reagents (Dynal Biotech ASA, Oslo, Norway), respectively (4, 5).

Activation of T-cells

The isolated CD4⁺ and CD8⁺ T-cells were counted on a Coulter A^CT diff hematology analyzer (Beckman Coulter, Miami, USA) and diluted to 10 × 10⁶ cells per mL. One mL (10 × 10⁶) of cells was incubated in a 25-mL tissue culture flask in RPMI 1640 medium containing 90 mg/dL glucose with no PHA (non-activation), and another one mL of cells was incubated for the same time period in another flask with 1 ng/mL PHA (for activation). The cells were maintained in 5% CO₂ and 95% air and incubated for 72 h, then the cells (10 × 10⁶) were placed in TRIZOL for RNA and protein extraction. According to the *de novo* emergence of gene expression of the insulin and other growth factor receptors and insulin signaling genes upon activation in normal CD4⁺ and CD8⁺ T-cells from normal individuals in our previous studies (8), we used the activated CD4⁺ and CD8⁺ T-cells for this study.

Isolation of RNA and proteins from T-cells and muscle tissues

Chloroform (0.2 mL) was added to the tubes containing T-cells (CD4⁺ or CD8⁺) or muscle tissues that had been placed in TRIZOL. The RNA and proteins were isolated as previously described (44, 45). RNA from each individual time point of each subject was probed with a microarray chip (8).

cRNA synthesis and labeling

The first and the second strand of cDNA were synthesized from 5–15 μg of total RNA using the SuperScript Double-Stranded cDNA Synthesis Kit (Gibco Life Technologies, Rockville, USA) and oligo-dT₂₄-T7 (5'-GGCCAGTGAATTGTAATACGACTCACTATA

GGGAGGCGG-3') primer according to the manufacturer's instructions. cRNA was synthesized and labeled with biotinylated UTP and CTP by *in vitro* transcription using the T7 promoter-coupled double-stranded cDNA as template and the T7 RNA Transcript Labeling Kit (ENZO Diagnostics Inc., Farmingdale, USA). The labeled cRNA was separated from unincorporated ribonucleotides by passing through a CHROMA SPIN-100 column (Clontech, Mountain View, USA) and precipitated at -20°C from 1 h to overnight as previously described (8).

Oligonucleotide array hybridization and analysis

The cRNA pellet was fragmented and hybridized to HG_U133A Plus 2 oligonucleotide arrays (Affymetrix, Santa Clara, USA) containing in excess of 400,000 full-length annotated nucleotide sequences to permit the simultaneous detection and quantitation of 31,000 human genes with additional probe sets designed to represent EST sequences for simultaneous detection and quantitation on one array. The arrays were then stained with phycoerythrin conjugated streptavidin (Molecular Probes Inc., Eugene, USA) and the fluorescence intensities were determined using a laser confocal scanner (Hewlett-Packard, Palo Alto, USA). The scanned images were analyzed using microarray software (Affymetrix). Sample loading and variations in staining were standardized by scaling the average of the fluorescent intensities of all genes on one array to constant target intensity (250) for all arrays used, all as we have previously described (8).

Quantitative RT-PCR analysis

The RNA extracted from the cells for gene expression analysis by the Affymetrix microarrays was analyzed by RT-PCR to quantitate the amount of mRNAs transcribed for the various genes to confirm the information from the microarrays. Reverse transcription of 250 ng of total RNA was performed using 125 U Multiscribe reverse transcriptase (Applied Biosystems, Foster City, USA). The cDNA was then analyzed by Applied Biosystems TaqMan low density arrays with 24 sets of genes. Each reaction consisted of 0.5–1 ng of cDNA per well in a final volume of 1 μL . Primer/probe sets were chosen from the pre-designed TaqMan gene expression assays. The cDNA was mixed with 2 \times TaqMan Universal Mastermix and 100 μL of the mixture was loaded into

each filling port. The plates were then centrifuged to distribute the mixture into the wells. Quantitative RT-PCR was performed on an Applied Biosystems 7900HT system. Absolute threshold cycle values (Ct values) were determined using SDS software (Applied Biosystems). The Ct values of the 23 mRNAs were normalized against the mean Ct value of the 18S rRNA ($\Delta\text{Ct}_{\text{test gene}} = \text{Ct}_{\text{test gene}} - \text{mean Ct}_{18\text{S}}$). The $\Delta\text{Ct}_{\text{test gene}}$ of normal subjects was then subtracted from the $\Delta\text{Ct}_{\text{test gene}}$ of diabetic subjects ($\Delta\Delta\text{Ct}_{\text{test gene}} = \Delta\text{Ct}_{\text{test gene diabetic}} - \Delta\text{Ct}_{\text{test gene normal}}$). The larger the $\Delta\Delta\text{Ct}_{\text{test gene}}$, the less the amount of mRNAs in diabetic subject cells (46).

Gene silencing to delineate gene function

RNAi was used for gene knockout to study the effect of decreases in mRNA expression levels. The CD4⁺ T-cells of normal subjects were transfected with Ambion's Silencer siRNAs (Ambion, Austin, USA) before activation of the cells, and mRNA knockout levels were measured using the same method as described above. An amount of 1 nM and 10 nM concentrations of Ambion's Silencer validated siRNAs for INSR (ID No. 31, 29, and 103467; RefSeq Accession NM.000208) or TNF α pre-designed siRNAs (ID No. 138754, 1338753, and 138752; RefSeq Accession NM.000594) was transfected into the T-cells prior to activation, respectively. The levels of mRNA for INSR, TNF α , and GLUT4 were assessed using RT-PCR with pre-designed TaqMan gene expression assays for INSR (NM.000208), TNF α (NM.000594), and GLUT4 (NM.001042), respectively. 18S rRNA was used to normalize from sample to sample. The percent relative gene expression to the control (no siRNA added) was determined (47).

Proteins translated

Proteins from muscle tissues and activated and non-activated CD4⁺ and CD8⁺ T-cells of normal and diabetic subjects were extracted using TRIZOL reagent according to the manufacturer's recommendations, and were then analyzed by 2D-PAGE and the Ciphergen PBSII SELDI-TOF MS System (Ciphergen Biosystems, Fremont, USA) (8).

2D-PAGE

Prior to 2D-PAGE separation, the proteins from the CD4⁺ and CD8⁺ T-cells and muscle tissues of normal and diabetic subjects extracted from TRIZOL reagent were solubilized in a standard rehydration solution containing urea, thiourea, dithiothreitol, CHAPS detergent, ampholytes, and protease/phosphatase inhibitors. Protein concentration in the rehydration buffer was determined by the 2-D Quant Kit (Amersham Biosciences, Piscataway, USA).

In the first dimension of 2D-PAGE, the proteins were subjected to isoelectric focusing (IEF), which separated the proteins according to their isoelectric points (pI). In the second dimension of 2D-PAGE, the proteins were separated by sodium dodecyl sulfate (SDS)-PAGE according to their MWs. A Multiphor II apparatus (Amersham) for IEF and a Protean Dodeca Plus apparatus (Bio-Rad, Hercules, USA) for SDS-PAGE were used in this study as previously described (48, 49).

For IEF of the protein mixtures, pre-cast gel strips with immobilized pH gradients were used (18 cm, pH 3–10). The total protein load was 100–200 μ g. For the second dimension of 2D-PAGE, self-cast polyacrylamide gels of 20×20 cm was used. After SDS-PAGE, the proteins in the 2D gels were visualized using the SYPRO Ruby fluorescence since it has a dynamic range of 1–10 ng and has an end-point reaction. The FX Molecular Imager (Bio-Rad) was used to scan the gels and create digitized images for computer-assisted spot pattern analysis, and the gel images were saved in an Adobe Photoshop format.

PF 2D system

The liquid-based 2D protein separation technology, the ProteomeLab PF 2D Protein Fractional System (Beckman Coulter, Fullerton, USA) for proteome analysis, was also used in this study because of the complex differences observed in the samples by 2D gels and the number of samples to be analyzed (50). The PF 2D system separated the proteins in complex mixtures in the first dimension using high performance chromatofocusing according to their pI, then automatically generated a sequence table for automated injection of the fractions into the second dimension where separation occurred according to hydrophobicity. Fractions were collected from the second dimension into a 96-well plate for analyses of the peaks by MS. The software allowed for comparison of

peaks of different samples, therefore the differences of protein peaks between samples were determined. This system could accommodate up to 5-mg protein, which allows for detection of proteins in lower concentrations.

MS analysis

MS analysis of the proteomes was performed using the Ciphergen PBSII SELDI-TOF MS System on gold (AU), hydrophobic (H50), anion exchange (Q10), and cation exchange (CM10) chip arrays (Ciphergen Biosystems). Differences between the cellular proteins of muscle tissues and activated CD4⁺ and CD8⁺ T-cells of normal and diabetic subjects were determined using Ciphergen MS software (8, 51).

Protein digestion for MALDI-TOF MS

The protein peaks collected in the wells of the 96-well plates were proteolytically digested to produce a mixture of peptides. Trypsin was used as the first choice, or if needed, proteases with different specificities, such as endoprotease Lys-C or Glu-C, were employed. The protein digests were extracted with a C18 minicolumn and were then analyzed on the MALDI-TOF mass spectrometer (Thermo Finnigan, San Jose, USA) (52).

Data analysis for gene expression

Data analysis was conducted using GeneChip operating software (Affymetrix) and GeneSifter (VizX Labs LLC, Seattle, USA) software following user guidelines. The signal intensity for each gene was calculated as the average intensity difference, represented by $[\Sigma(\text{PM} - \text{MM})/(\text{the number of probe pairs})]$, where PM and MM denote perfect match and mismatch probes, respectively. To identify genes that are differentially expressed in T-cells between newly diagnosed T2DM subjects and normal subjects, the following filtering method was used. Affymetrix detection calls were used to remove genes that did not have all “Present” calls for each sample in at least one group. Genes that met these criteria and showed at least a 1.5-fold change between any of the groups were then subjected to the analysis of variance (ANOVA). Raw *p*-values from ANOVA were adjusted using the method of Benjamini and Hochberg (53) to calculate a false discovery rate. A false discovery rate of less than or equal to 1% was then applied to generate a list of differentially expressed genes. Hierarchical

clustering was used to visualize the filtered gene list and identify patterns of gene expression. K-medoids clustering was used to partition the filtered gene list based on expression pattern. Clusters showing gene expression patterns of interest were then examined on a gene-by-gene basis using the annotation from UniGene and Entrez Gene databases. Additionally, z-score analysis (54) was used for the GO and KEGG pathway terms associated with the genes in the cluster to identify biological themes associated with a cluster of interest. As our main focus of pathways was on insulin receptor, insulin signaling, glucose transport, glucose and lipid metabolism, and immune function pathways, we specifically analyzed these pathways in this study using Ingenuity software.

SELDI-TOF MS

Ciphergen ProteinChip 3.1 software was used to calculate and subtract the background, and Biomarker Wizard software was used to detect peaks with a signal to noise ratio of 5 or greater, to match peaks within a mass window of 0.3%, and to perform statistical analysis using a t-test to determine significant differences in protein expression. Data were exported to Statview 5.0 software to perform ANOVA and evaluate the significance of multiple comparisons. These analyses defined the patterns of protein expression that consistently differed in muscle tissues and activated CD4⁺ and CD8⁺ T-cells between normal and diabetic subjects (8).

2D-PAGE image analysis

The TIFF images of the scanned gels were imported into PDQuest image analysis software (version 7.1, Bio-Rad), which allows the intensities of protein spots in many gels to be compared at once when composite gels are created, and advanced statistical analyses were performed. The protein spots were detected using the automated spot detection feature, and the correction for undetected or incorrectly detected spots or artifacts was done by visual inspection using a stringent definition of spots in order to avoid collecting data from very faint spots that tend to have substantial intersample variability and reproducibility. The spot intensity (the integration of optical density over the spot's area) was determined, and differential data analysis was performed to quantify spot variations from gel to gel. Statistical analysis, using univariate and multivariate statistical techniques, was performed

on the groups of proteins from normal and diabetic subjects to determine the differences in protein expression between the two kinds of subjects (48, 49).

Acknowledgements

We thank Guillermo Umpierrez, Hooman Oktaei, Ruben Cuervo, Ramona Pierce, Mustafa Dabbous, John Crisler, and Divyen Patel (Genome Explorations Inc.) for running the microarrays and microarray data analyses, as well as nurses and staff of the UTHSC General Clinical Research Center. This study was supported in part by USPHS General Clinical Research Center (Grant No. RR0211) of the National Institutes of Health, USA.

Authors' contributions

FBS conceived the idea of using this approach, supervised the project, recruited the patients, collected the datasets, supervised the data analyses, and prepared the manuscript. AEK assisted in screening the patients, assisted in data presentation, and co-wrote the manuscript. Both authors read and approved the final manuscript.

Competing interests

The authors have declared that no competing interests exist.

References

1. Helderman, J.H. 1981. Role of insulin in the intermediary metabolism of the activated thymic-derived lymphocyte. *J. Clin. Invest.* 67: 1636-1642.
2. Buffington, C.K., *et al.* 1986. Phytohemagglutinin (PHA) activated human T-lymphocytes: concomitant appearance of insulin binding, degradation and insulin-mediated activation of pyruvate dehydrogenase (PDH). *Biochem. Biophys. Res. Commun.* 134: 412-419.
3. Ercolani, L., *et al.* 1985. Insulin-induced desensitization at the receptor and postreceptor level in mitogen-activated human T-lymphocytes. *Diabetes* 34: 931-937.
4. Stentz, F.B. and Kitabchi, A.E. 2003. Activated T lymphocytes in Type 2 diabetes: implications for *in vitro* studies. *Curr. Drug Targets* 4: 493-503.
5. Stentz, F.B. and Kitabchi, A.E. 2004. *De novo* emergence of growth factor receptors in activated human

- CD4⁺ and CD8⁺ T lymphocytes. *Metabolism* 53: 117-122.
6. Kitabchi, A.E., *et al.* 1991. Role of adrenal and gonadal androgens in insulin action and metabolism. *Folia Endocrinologica Japonica* 67: 203-213.
 7. Buffington, C.K., *et al.* 1991. Opposing actions of dehydroepiandrosterone and testosterone on insulin sensitivity. *In vivo* and *in vitro* studies of hyperandrogenic females. *Diabetes* 40: 693-700.
 8. Stentz, F.B. and Kitabchi, A.E. 2004. Transcriptome and proteome expression in activated human CD4 and CD8 T-lymphocytes. *Biochem. Biophys. Res. Commun.* 324: 692-696.
 9. Kitabchi, A.E., *et al.* 2004. Diabetic ketoacidosis induces *in vivo* activation of human T-lymphocytes. *Biochem. Biophys. Res. Commun.* 315: 404-407.
 10. Stentz, F.B., *et al.* 2004. Proinflammatory cytokines, markers of cardiovascular risks, oxidative stress, and lipid peroxidation in patients with hyperglycemic crises. *Diabetes* 53: 2079-2086.
 11. Stentz, F.B. and Kitabchi, A.E. 2005. Hyperglycemia-induced activation of human T-lymphocytes with *de novo* emergence of insulin receptors and generation of reactive oxygen species. *Biochem. Biophys. Res. Commun.* 335: 491-495.
 12. Accili, D. and Kanno, H. 1999. The mechanism of insulin action. In *Atlas of Clinical Endocrinology*, Volume 2, *Diabetes* (eds. Korenman, S.G. and Kahn, C.R.), pp. 12-28. Current Medicine, Inc., Philadelphia, USA.
 13. Cheatham, B. and Kahn, C.R. 1996. The biochemistry of insulin action. In *Diabetes Mellitus: A Fundamental and Clinical Text* (eds. LeRoith, D., *et al.*), pp. 139-147. Lippincott Williams & Wilkins, Philadelphia, USA.
 14. White, M. and Fisher, T.L. 2002. The mechanisms of insulin action. In *Atlas of Diabetes* (ed. Skyler, J.S.), second edition, pp. 15-26. Lippincott Williams & Wilkins, Philadelphia, USA.
 15. Saltiel, A.R. and Kahn, C.R. 2001. Insulin signalling and the regulation of glucose and lipid metabolism. *Nature* 414: 799-806.
 16. DeFronzo, R.A. and Ferrannini, E. 1991. Insulin resistance, a multifaceted syndrome responsible for NIDDM, obesity, hypertension, dyslipidemia, and atherosclerotic cardiovascular disease. *Diabetes Care* 14: 173-194.
 17. Wong, J.A., *et al.* 2001. Insulin-independent, MAPK-dependent stimulation of NKCC activity in skeletal muscle. *Am. J. Physiol. Regul. Integr. Comp. Physiol.* 281: R561-571.
 18. Gosmanov, A.R., *et al.* 2004. Impaired expression and insulin-stimulated phosphorylation of Akt-2 in muscle of obese patients with atypical diabetes. *Am. J. Physiol. Endocrinol. Metab.* 287: E8-15.
 19. Goldstein, B.J., *et al.* 2005. Redox paradox: insulin action is facilitated by insulin-stimulated reactive oxygen species with multiple potential signaling targets. *Diabetes* 54: 311-321.
 20. Haffner, S.J. and Cassells, H. 2003. Hyperglycemia as a cardiovascular risk factor. *Am. J. Med.* 115: 6S-11S.
 21. Jialal, I., *et al.* 1985. Characterization of the receptors for insulin and the insulin-like growth factors on micro- and macrovascular tissues. *Endocrinology* 117: 1222-1229.
 22. Kondo, T. and Kahn, C.R. 2004. Altered insulin signaling in retinal tissue in diabetic states. *J. Biol. Chem.* 279: 37997-38006.
 23. Mohanty, P., *et al.* 2000. Glucose challenge stimulates reactive oxygen species (ROS) generation by leukocytes. *J. Clin. Endocrinol. Metab.* 85: 2970-2973.
 24. Sheetz, M.J. and King, G.L. 2002. Molecular understanding of hyperglycemia's adverse effects for diabetic complications. *JAMA* 288: 2579-2588.
 25. Wei, M., *et al.* 1998. Effects of diabetes and level of glycemia on all-cause and cardiovascular mortality. The San Antonio Heart Study. *Diabetes Care* 21: 1167-1172.
 26. Stentz, F.B. and Kitabchi, A.E. 2006. Palmitic acid-induced activation of human T-lymphocytes and aortic endothelial cells with production of insulin receptors, reactive oxygen species, cytokines, and lipid peroxidation. *Biochem. Biophys. Res. Commun.* 346: 721-726.
 27. Kitabchi, A.E., *et al.* 1979. Accelerated insulin degradation: an alternate mechanism for insulin resistance. *Diabetes Care* 2: 414-417.
 28. Duckworth, W.C., *et al.* 1979. Initial site of insulin cleavage by insulin protease. *Proc. Natl. Acad. Sci. USA* 76: 635-639.
 29. Kitabchi, A.E., *et al.* 1990. Insulin synthesis, proinsulin and C-peptide. In *Diabetes Mellitus* (eds. Porte, D., *et al.*), 4th edition, pp. 71-88. McGraw-Hill Companies, Inc.
 30. Zhao, L., *et al.* 2004. Insulin-degrading enzyme as a downstream target of insulin receptor signaling cascade: implications for Alzheimer's disease intervention. *J. Neurosci.* 24: 11120-11126.
 31. Stentz, F.B., *et al.* 1989. Identification of insulin intermediates and sites of cleavage of native insulin by insulin protease from human fibroblasts. *J. Biol. Chem.* 264: 20275-20282.
 32. Mahadev, K., *et al.* 2004. Integration of multiple downstream signals determines the net effect of insulin on MAP kinase vs. PI 3'-kinase activation: potential role of insulin-stimulated H₂O₂. *Cell. Signal.* 16: 323-331.
 33. Zierath, J.R., *et al.* 2000. Insulin action and insulin resistance in human skeletal muscle. *Diabetologia* 43:

- 821-835.
34. Maddux, B.A., *et al.* 2006. Overexpression of the insulin receptor PC-1/ENPP1 induces insulin resistance and hyperglycemia. *Am. J. Physiol. Endocrinol. Metab.* 290: E746-749.
 35. Aljada, A., *et al.* 2002. Tumor necrosis factor- α inhibits insulin-induced increase in endothelial nitric oxide synthase and reduces insulin receptor content and phosphorylation in human aortic endothelial cells. *Metabolism* 51: 487-491.
 36. Solomon, S.S., *et al.* 2005. Proteome of H-411E (liver) cells exposed to insulin and tumor necrosis factor- α : analysis of proteins involved in insulin resistance. *J. Lab. Clin. Med.* 145: 275-283.
 37. Haussler, M.R., *et al.* 1997. The vitamin D hormone and its nuclear receptor: molecular actions and disease states. *J. Endocrinol.* 154: 557-573.
 38. Pittas, A.G., *et al.* 2007. The role of vitamin D and calcium in type 2 diabetes. A systematic review and meta-analysis. *J. Clin. Endocrinol. Metab.* 92: 2017-2029.
 39. Nakae, J., *et al.* 2001. Insulin regulation of gene expression through the forkhead transcription factor Foxo1 (Fkhr) requires kinases distinct from Akt. *Biochemistry* 40: 11768-11776.
 40. Ross, R. 1999. Atherosclerosis—an inflammatory disease. *N. Engl. J. Med.* 340: 115-126.
 41. Bar, R.S., *et al.* 1988. Insulin, insulin-like growth factors, and vascular endothelium. *Am. J. Med.* 85: 59-70.
 42. Gosmanov, A.R., *et al.* 2005. *De novo* emergence of insulin-stimulated glucose uptake in human aortic endothelial cells incubated with high glucose. *Am. J. Physiol. Endocrinol. Metab.* 290: E516-522.
 43. Report of the expert committee on the diagnosis and classification of diabetes mellitus. 1997. *Diabetes Care* 20: 1183-1197.
 44. Stentz, F.B., *et al.* 1985. Characterization of insulin-degrading activity of intact and subcellular components of human fibroblasts. *Endocrinology* 116: 926-934.
 45. Meduri, G.U., *et al.* 2002. Prolonged methylprednisolone treatment suppresses systemic inflammation in patients with unresolving acute respiratory distress syndrome: evidence for inadequate endogenous glucocorticoid secretion and inflammation-induced immune cell resistance to glucocorticoids. *Am. J. Respir. Crit. Care Med.* 165: 983-991.
 46. Antonov, J., *et al.* 2005. Reliable gene expression measurements from degraded RNA by quantitative real-time PCR depend on short amplicons and a proper normalization. *Lab. Invest.* 85: 1040-1050.
 47. Shah, J.K., *et al.* 2007. sIR: siRNA Information Resource, a web-based tool for siRNA sequence design and analysis and an open access siRNA database. *BMC Bioinformatics* 8: 178.
 48. Gerling, I.C., *et al.* 2006. New data analysis and mining approaches identify unique proteome and transcriptome markers of susceptibility to autoimmune diabetes. *Mol. Cell. Proteomics* 5: 293-305.
 49. Zhan, X. and Desiderio, D. 2003. Spot volume vs. amount of protein loaded onto a gel: a detailed, statistical comparison of two gel electrophoresis systems. *Electrophoresis* 24: 1818-1833.
 50. Kachman, M.T., *et al.* 2002. A 2-D liquid separations/mass mapping method for interlysate comparison of ovarian cancers. *Anal. Chem.* 74: 1779-1791.
 51. Issaq, H.J., *et al.* 2002. The SELDI-TOF MS approach to proteomics: protein profiling and biomarker identification. *Biochem. Biophys. Res. Commun.* 292: 587-592.
 52. Giorgianni, F., *et al.* 2004. Identification and characterization of phosphorylated proteins in the human pituitary. *Proteomics* 4: 587-598.
 53. Reiner, A., *et al.* 2003. Identifying differentially expressed genes using false discovery rate controlling procedures. *Bioinformatics* 19: 368-375.
 54. Doniger, S.W., *et al.* 2003. MAPPFinder: using Gene Ontology and GenMAPP to create a global gene-expression profile from microarray data. *Genome Biol.* 4: R7.